

The effect of die geometry on the microstructure of indirect squeeze cast and gravity die cast 7050 (Al-6.2Zn-2.3Cu-2.3Mg) wrought Al alloy

S-W KIM, G. DURRANT*, J-H LEE**, B. CANTOR*

Chonbuk National University, Chonju, Korea 562 170

**Oxford Centre for Advanced Materials and Composites, Department of Materials, University of Oxford, Parks Road, Oxford OX1 3PH, UK*

***RASOM, Chungnam National University, Taedok Science Town, Taejon 305-764, Korea*

The indirect squeeze casting process has been used to cast a 7050 (Al-6.2Zn-2.3Cu-2.3Mg) wrought Al alloy to near-net shape with excellent die replication. Defects which occur with gravity casting, in particular (1) shrinkage pipe, (2) macro-porosity and (3) hot-tearing, are largely removed by squeeze casting, although regions of macro-porosity can re-appear when thick sections are fed through substantially thinner sections. Squeeze casting results in a considerable refinement of microstructure compared to gravity casting due to a marked decrease in solidification time. The decrease in solidification time is caused by intimate contact between the pressurised melt and the die, which leads to an increase in the heat transfer coefficient. Decreasing the section thickness also results in a refinement of the microstructure due to a reduction in solidification time. © 1999 Kluwer Academic Publishers

1. Introduction

The squeeze casting process, where solidification takes place under a high applied pressure, has a number of advantages over sand casting and gravity die casting for Al alloys. The high pressure leads to excellent feeding of solidification shrinkage and a refined microstructure due to high cooling rates, both of which result in excellent mechanical properties [1]. Near-net shape components can be manufactured with good surface finish and dimensional control at production rates comparable to a conventional pressure die caster [2]. Squeeze casting can also be used to cast Al alloys of wrought composition to shape, to give high strength, ductile components, although problems caused by the long freezing range of these alloys such as hot-tearing, shrinkage porosity and macrosegregation have not yet been extensively investigated [1, 3].

There are two main types of squeeze casting, direct and indirect, which differ in the manner in which the melt is fed into the tool steel die [2, 3]. In the case of direct squeeze casting, the melt is poured directly into the top of an open die, and a hydraulic ram is moved down into contact with the melt to apply the pressure [3]. Direct squeeze casting has two main drawbacks: (1) There is no control over the die filling stage, leading to turbulent flow and the entrainment of brittle surface oxide films [4]; and (2) there is an inherent time delay after melt pouring prior to pressurisation with the ram, leading to significant solidification under gravity casting conditions [5, 6]. Indirect squeeze casting overcomes these limitations by injecting the melt into the bottom of the die cavity with a hydraulic ram so that fluid flow

can be controlled via the injection speed, and by commencing pressurisation as soon as the die is filled.

In this paper we present results on the squeeze casting of a high strength 7050 (Al-6.2Zn-2.3Cu-2.3Mg) wrought Al alloy using an experimental indirect squeeze casting unit. The results are compared with gravity castings manufactured under comparable conditions. The resultant macro- and microstructures for a range of die geometries are discussed in terms of the measured cooling behaviour during solidification.

2. Experimental techniques

2.1. Material

The material used in this study was 7050 (Al-6.2 wt % Zn-2.3 wt % Cu-2.3 wt % Mg) wrought Al alloy, supplied by Alcan International. The alloy is commonly used in the wrought condition for aircraft structural parts due to its high strength and fracture toughness, combined with a good resistance to fatigue damage and stress-corrosion cracking. The alloy has a long freezing range of $\sim 175^\circ\text{C}$ due to a low melting point eutectic reaction at $\sim 470^\circ\text{C}$, and a high liquidus temperature of $\sim 645^\circ\text{C}$ [7].

2.2. Casting methods

The experimental indirect squeeze casting unit consisted of a Mackey Bowley 100 ton hydraulic press, a Cheltenham 12 kW induction heater, and a Schlumberger 10 Hz data logger. Fig. 1 shows a schematic of the ram and die arrangement. The ram was fixed to the

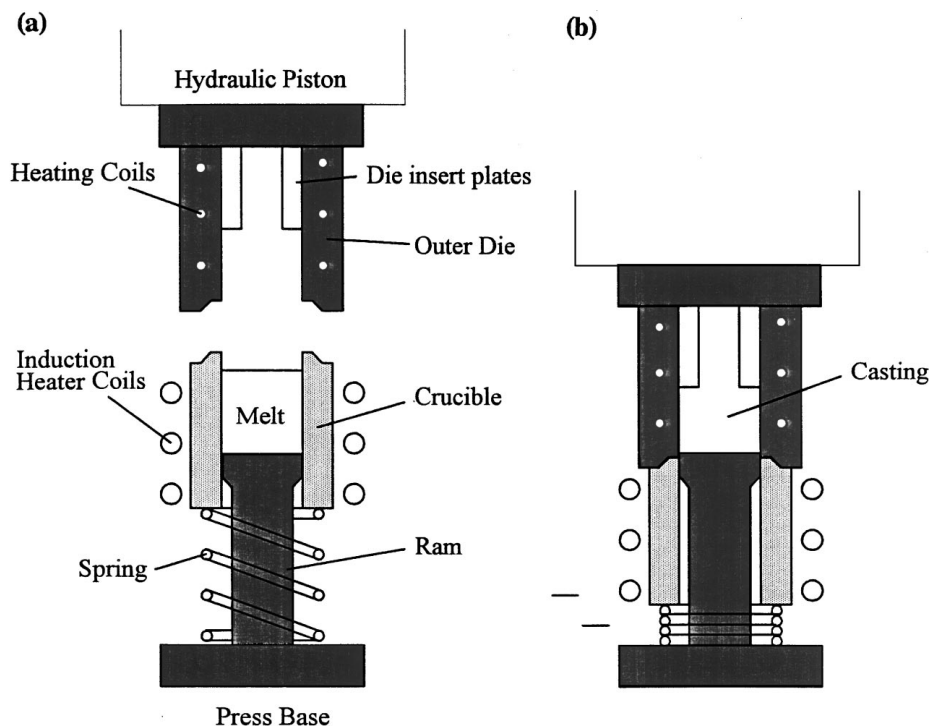


Figure 1 Schematic diagram of the experimental indirect squeeze unit.

base of the press and a close fitting graphite crucible was placed around the ram, supported from below by a spring. The induction heater coils were located around the crucible. The H13 tool steel die was fixed to the bottom of the main hydraulic ram, with the opening to the die cavity pointing downwards. A series of immersion heaters was inserted in the die to allow pre-heating prior to casting. In a typical squeeze casting cycle, a 7050 Al alloy charge was placed in the crucible on top of the ram, Fig. 1a, and was then melted by heating to $\sim 800^\circ\text{C}$. The hydraulic ram with the attached die pre-heated to 300°C was moved downwards at a rate of 21 mm s^{-1} into contact with the crucible. As the die continued to move downwards, the crucible was pushed down against the spring and the melt was injected into the die cavity, with a pressure of 50 MPa applied to the melt once the die cavity was filled, Fig. 1b. When the melt had completely solidified, the pressure was released and the die arrangement disassembled to remove the billet.

The cavity of the die bore was 50 mm in diameter, with close fitting tolerances against the 50 mm diameter ram. Die inserts were placed within the main die cavity to produce more complex geometries. Figs 2a and b show the simplest geometry studied, which contained die inserts to produce a square cross section $20\text{ mm} \times 20\text{ mm}$ and 60 mm in length, with an additional 50 mm diameter biscuit from the die bore. Additional die inserts 20 mm in length were used to reduce the thickness of the cross-section half-way along its length to 10, 5 and 2 mm, see Figs 2c–e, although the width was constant at 20 mm. Four casting geometries were therefore studied with middle section thicknesses of 20, 10, 5 and 2 mm. Fig. 2c shows the nomenclature used to describe the different sections of each billet, namely the biscuit, base, middle, and end sections.

Four thermocouples were used for each casting, three located at the centre of the cross-section of the die cavity in the base, middle and end sections, see Fig. 2d, and one located in the die.

For comparison with indirect squeeze cast billets, a series of gravity die cast billets was manufactured by removing the die from the hydraulic ram, inverting the die, and pouring the 7050 Al alloy melt directly into the die cavity, using a die pre-heat temperature of 300°C and a melt temperature of $\sim 800^\circ\text{C}$.

2.3. Microstructural analysis

Each casting was sectioned longitudinally at mid-width using a diamond cut-off wheel. One side was ground on SiC paper to 1200 grit to reveal the macrostructure. The other side was prepared for optical microscopy by sectioning, mounting in Bakelite, grinding on SiC paper, polishing with 6 and $1\ \mu\text{m}$ diamond slurry, and finally finishing with colloidal silica.

3. Results

3.1. Cooling curves

Fig. 3 shows cooling curves for gravity cast 7050 alloy with middle section thicknesses of 20, 10, 5 and 2 mm. In the case of a middle section thickness of 20 mm, Fig. 3a, the temperature at the base, middle and end thermocouple locations increased to $\sim 760^\circ\text{C}$ when the melt was poured at $\sim 5\text{ s}$, after which the cooling rate was $\sim 28^\circ\text{C s}^{-1}$ down to a thermal arrest at $\sim 625^\circ\text{C}$ due to the onset of solidification. The subsequent cooling rate was greatest at the end section and lowest at the base section. In a previous publication [7], differential scanning calorimetry (DSC) studies on the 7050 alloy have shown that the final solidification temperature is

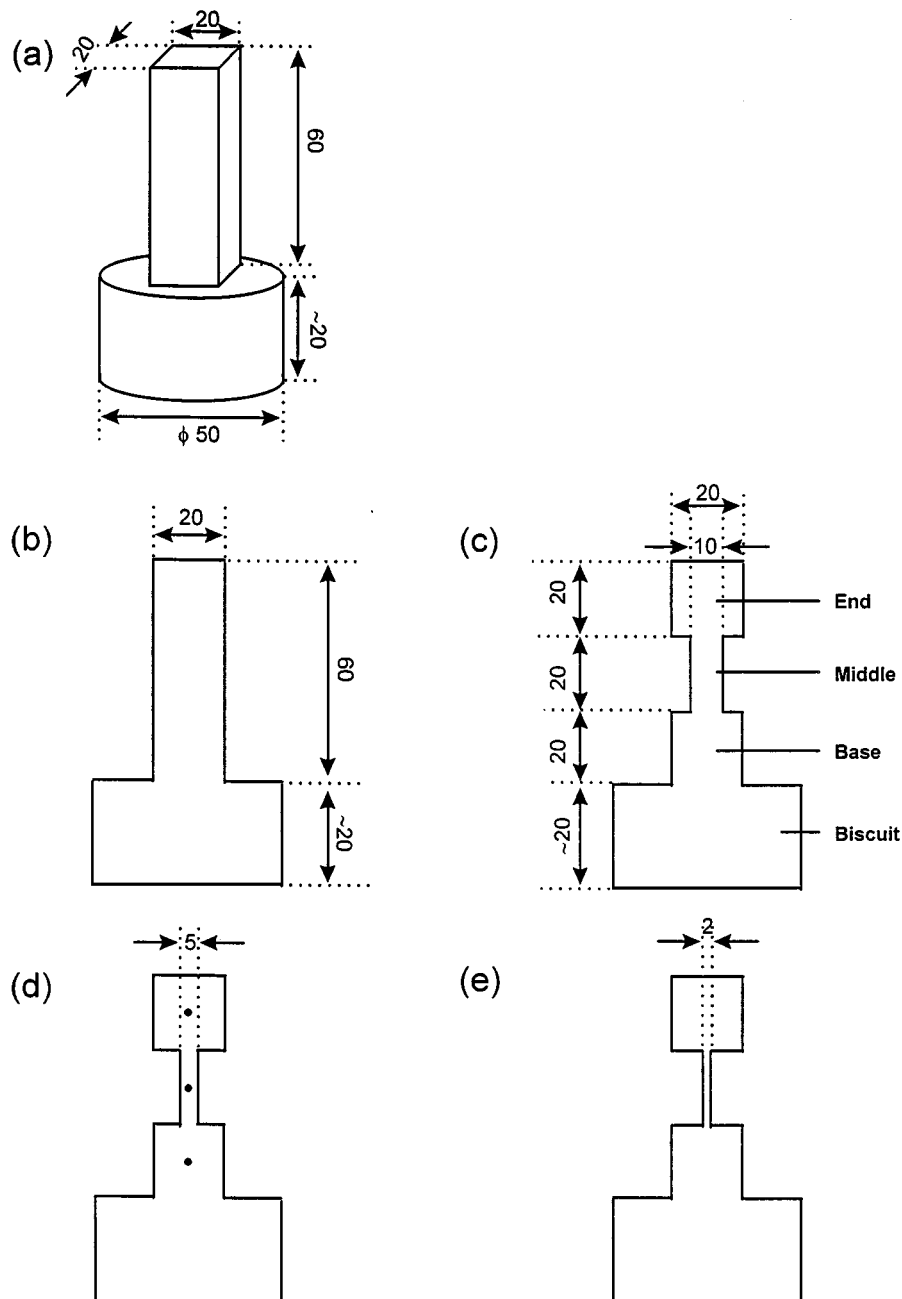


Figure 2 (a) Schematic diagram of the indirect squeeze cast billets, and longitudinal sections through the billets at mid-width for middle section thicknesses of (b) 20 mm, (c) 10 mm, (d) 5 mm and (e) 2 mm. The nomenclature used to describe the biscuit, base, middle and end sections is shown in (c), and the thermocouple locations are shown in (d).

~470 °C, and this temperature has been used to calculate solidification times after melt pouring and after the onset of solidification, as shown in Table I. The solidification time after melt pouring decreased from ~52.2 s at the base to ~18.2 s at the end, with corresponding solidification times after the onset of solidification of ~45.4 and ~15.0 s. Decreasing the thickness of the middle section generally had a relatively small effect on the cooling rate at the base and end sections, but caused a significant increase in cooling rate at the middle section, Figs 3a–d, with a corresponding decrease in solidification time, see Table I. Fig. 4 shows the solidification time at the middle section after melt pouring and after the onset of solidification as a function of the middle section thickness, which decreased from ~29.7 and ~25.2 s respectively for a

middle section thickness of 20 mm, to ~12.4 and ~11.2 s respectively for a middle section thickness of 2 mm.

TABLE I Solidification times for gravity cast 7050 alloy after melt pouring and after the onset of solidification for middle section thicknesses of 20, 10, 5 and 2 mm

Middle section thickness (mm)	Solidification time after melt pouring (s)			Solidification time after the onset of solidification (s)		
	Base	Middle	End	Base	Middle	End
20	52.2	29.7	18.2	45.4	25.2	15.0
10	53.0	—	20.5	47.8	—	17.6
5	50.4	21.0	24.7	45.7	18.6	23.4
2	43.8	12.4	43.6	40.0	11.2	41.1

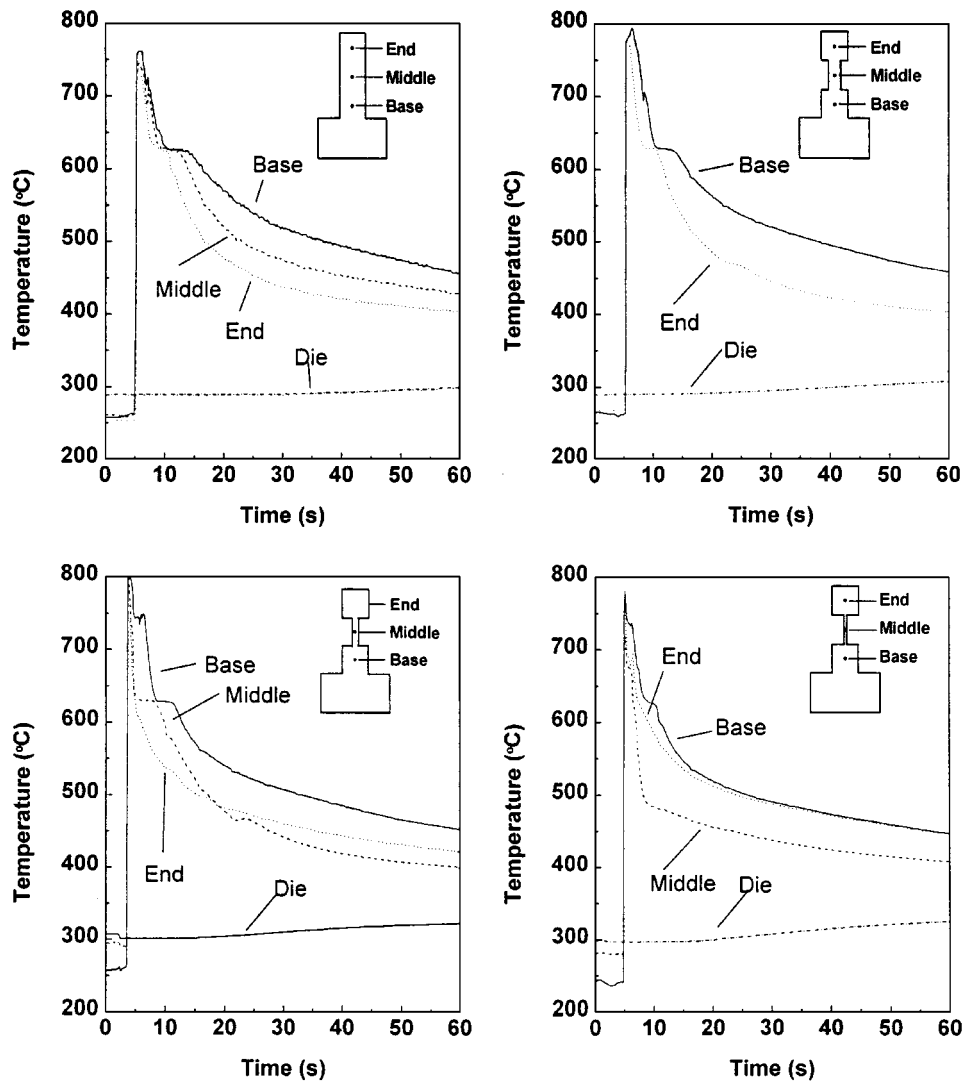


Figure 3 Cooling curves for gravity cast 7050 alloy with middle section thicknesses of (a) 20 mm, (b) 10 mm, (c) 5 mm and (d) 2 mm.

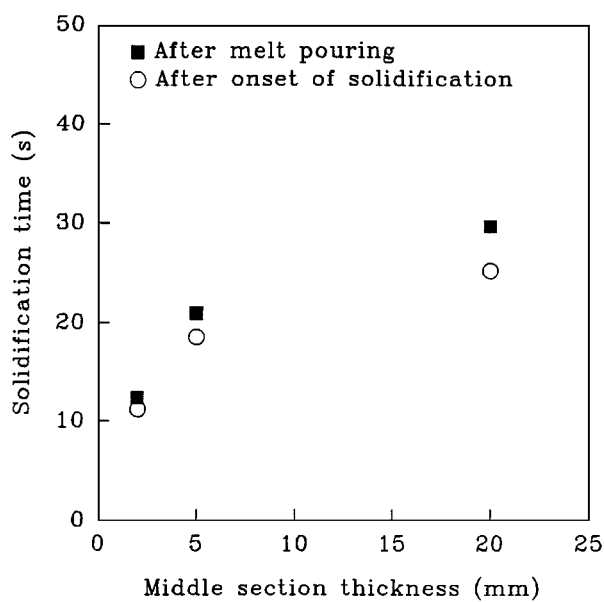


Figure 4 Solidification times at the middle section for gravity cast 7050 alloy after melt pouring and after the onset of solidification as a function of middle section thickness.

Fig. 5 shows cooling curves for indirect squeeze cast 7050 alloy with middle section thicknesses of 20, 10, 5 and 2 mm. In the case of a middle section thickness of 20 mm, Fig. 5a, the temperature after melt injection at ~ 2 s increased to $\sim 700^\circ\text{C}$, and the subsequent cooling rate prior to the onset of solidification of $\sim 120^\circ\text{C s}^{-1}$ was substantially greater than the cooling rate of $\sim 28^\circ\text{C s}^{-1}$ for gravity casting with a middle section thickness of 20 mm, Fig. 3a. The thermal arrest time at the onset of solidification for squeeze casting was less than half the time for squeeze casting, with a higher subsequent cooling rate. The solidification time at the middle section after melt injection was ~ 7.8 s for squeeze casting, compared with ~ 29.7 s for gravity casting, Tables I and II, with corresponding solidification times after the onset of solidification of ~ 7.3 and ~ 25.2 s respectively. Decreasing the middle section thickness resulted in a substantial decrease in the solidification time at the middle section, Fig. 6 and Table II, with a decrease in solidification time after melt injection from ~ 7.8 s for a section thickness of 20 mm to ~ 1.3 s for a section thickness of 2 mm, with corresponding solidification times after the onset of solidification of ~ 7.3 and ~ 1.1 s respectively.

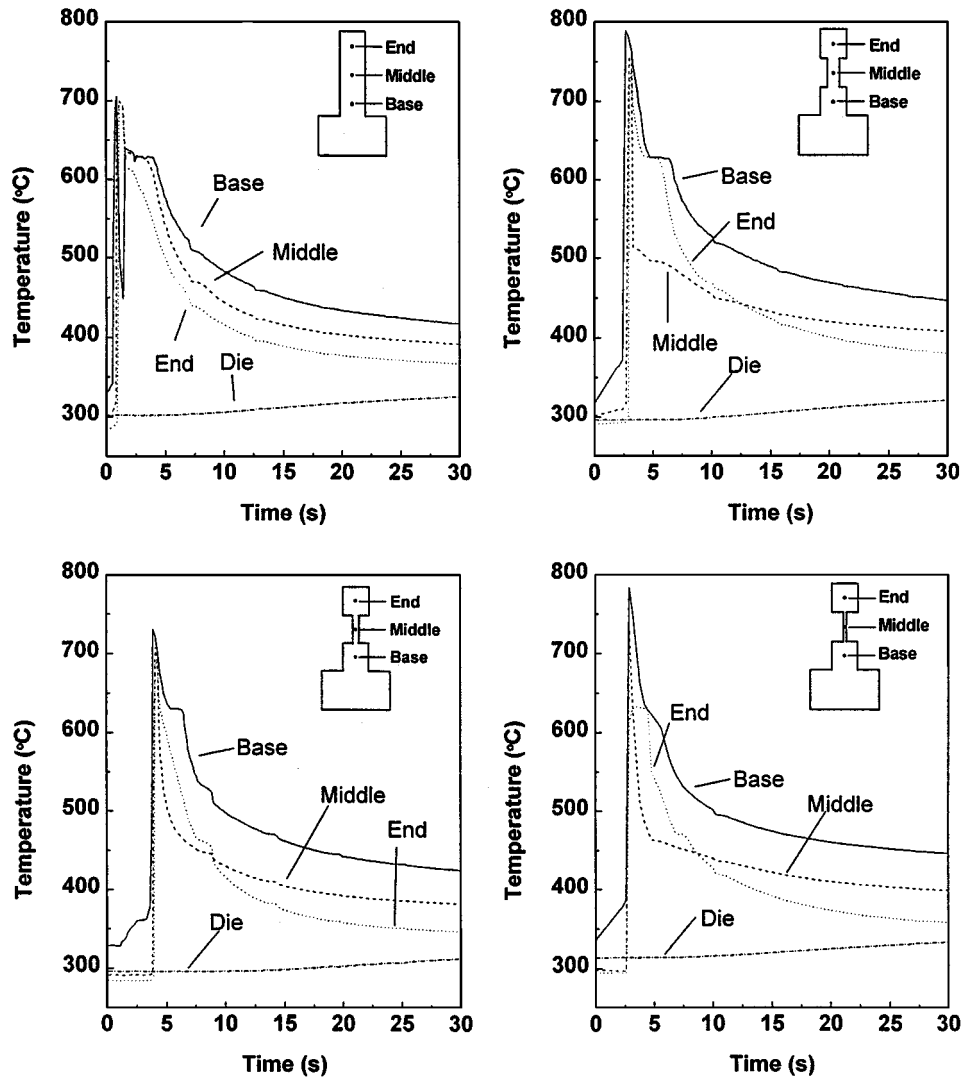


Figure 5 Cooling curves for indirect squeeze cast 7050 alloy with middle section thicknesses of (a) 20 mm, (b) 10 mm, (c) 5 mm and (d) 2 mm.

3.2. Die replication and macrostructure

Figs 7a and b show gravity and squeeze cast 7050 Al alloy billets with section thickness of 20, 10, 5 and 2 mm. With the gravity cast billets, Fig. 7a, die replication was relatively poor, with shrinkage away from the flat die surfaces and considerable rounding of the vertices. However, with the squeeze cast billets, Fig. 7b, die replication was excellent, with flat surfaces and well defined vertices.

Figs 8a and b show the macrostructure of sections taken at the mid-width of gravity and squeeze cast billets. With the gravity cast billets, Fig. 8a, three main

TABLE II Solidification times for indirect squeeze cast 7050 alloy after melt injection and after the onset of solidification for middle section thicknesses of 20, 10, 5 and 2 mm

Middle section thickness (mm)	Solidification time after melt injection (s)			Solidification time after the onset of solidification (s)		
	Base	Middle	End	Base	Middle	End
20	12.7	7.8	5.7	12.2	7.3	5.2
10	19.3	6.3	10.2	17.7	6.0	8.9
5	11.0	2.6	3.7	9.8	2.4	3.5
2	8.9	1.3	3.5	7.5	1.1	3.2

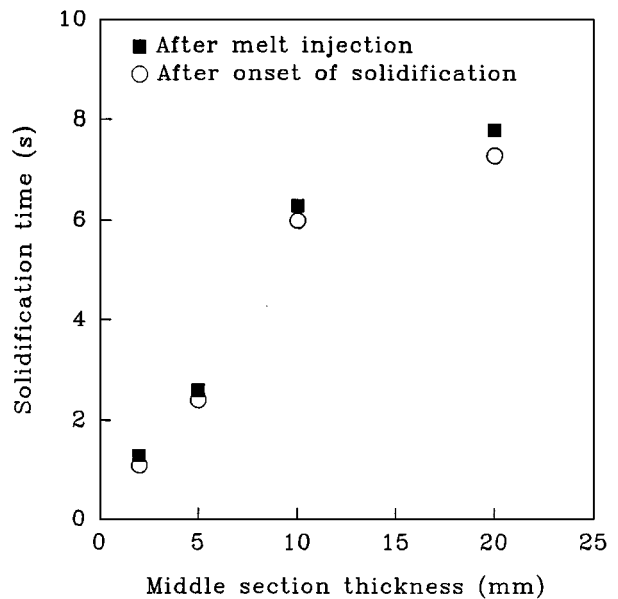


Figure 6 Solidification times at the middle section for indirect squeeze cast 7050 alloy after melt injection and after the onset of solidification as a function of middle section thickness.

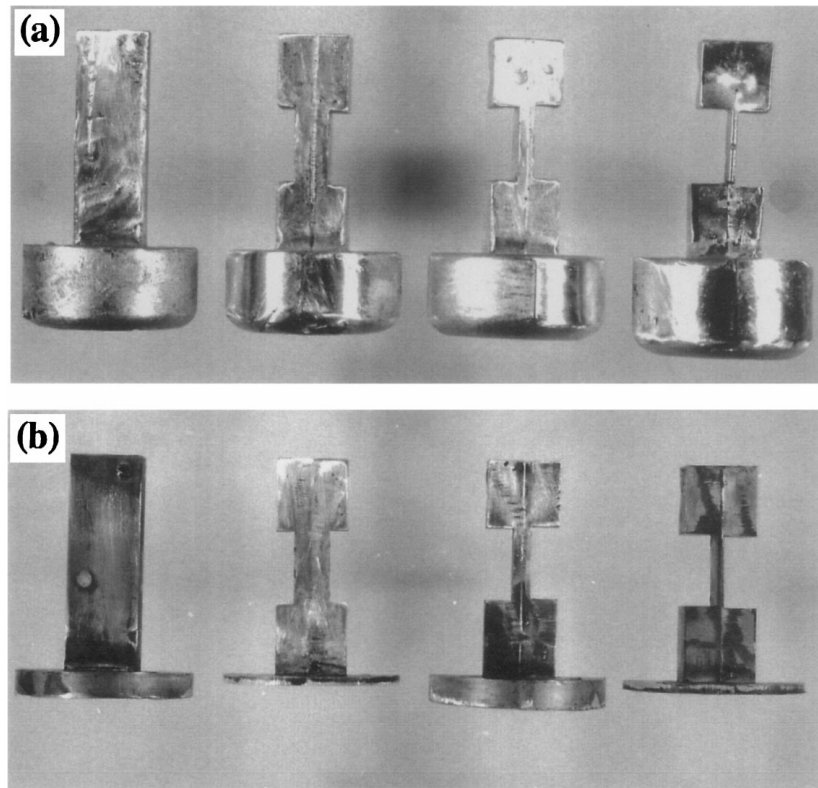


Figure 7 Photographs of 7050 billets with section thicknesses of 20, 10, 5 and 2 mm manufactured by (a) gravity casting and (b) indirect squeeze casting.

types of defect were observed: (1) The biscuit of each billet contained a shrinkage pipe defect; (2) large shrinkage voids up to 10 mm in length were present in the end sections of the billets with middle section

thicknesses of 5 and 2 mm, see Fig. 9a; and (3) hot-tear cracks were observed across the thickness of the billet where the middle section joins the base section for billets with middle section thicknesses of 10, 5 and

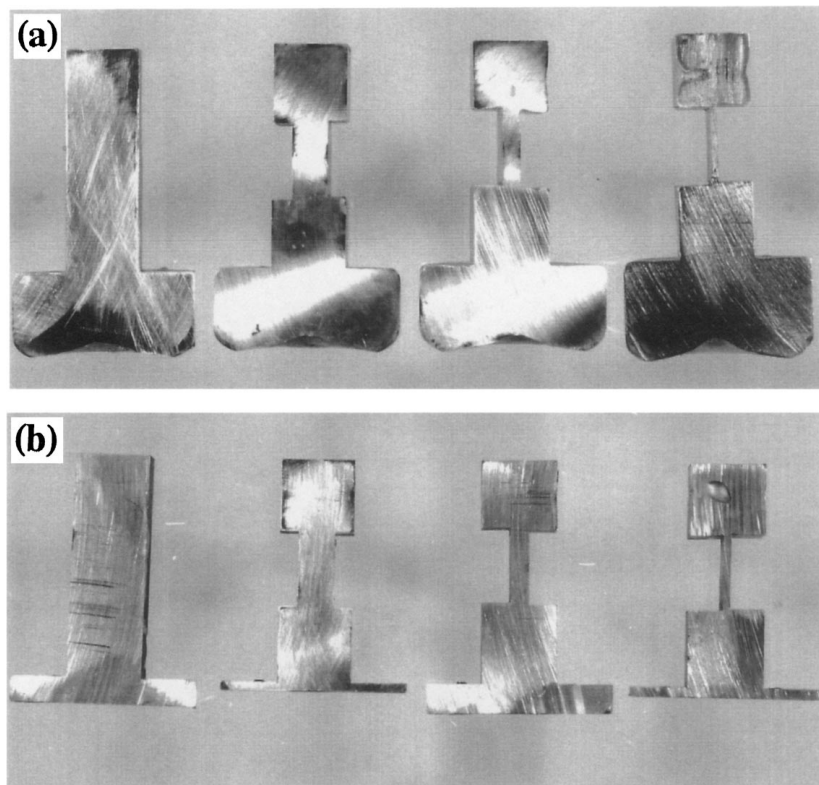


Figure 8 Macrostructure of longitudinal sections at mid-width from 7050 billets with section thicknesses of 20, 10, 5 and 2 mm manufactured by (a) gravity casting and (b) indirect squeeze casting.

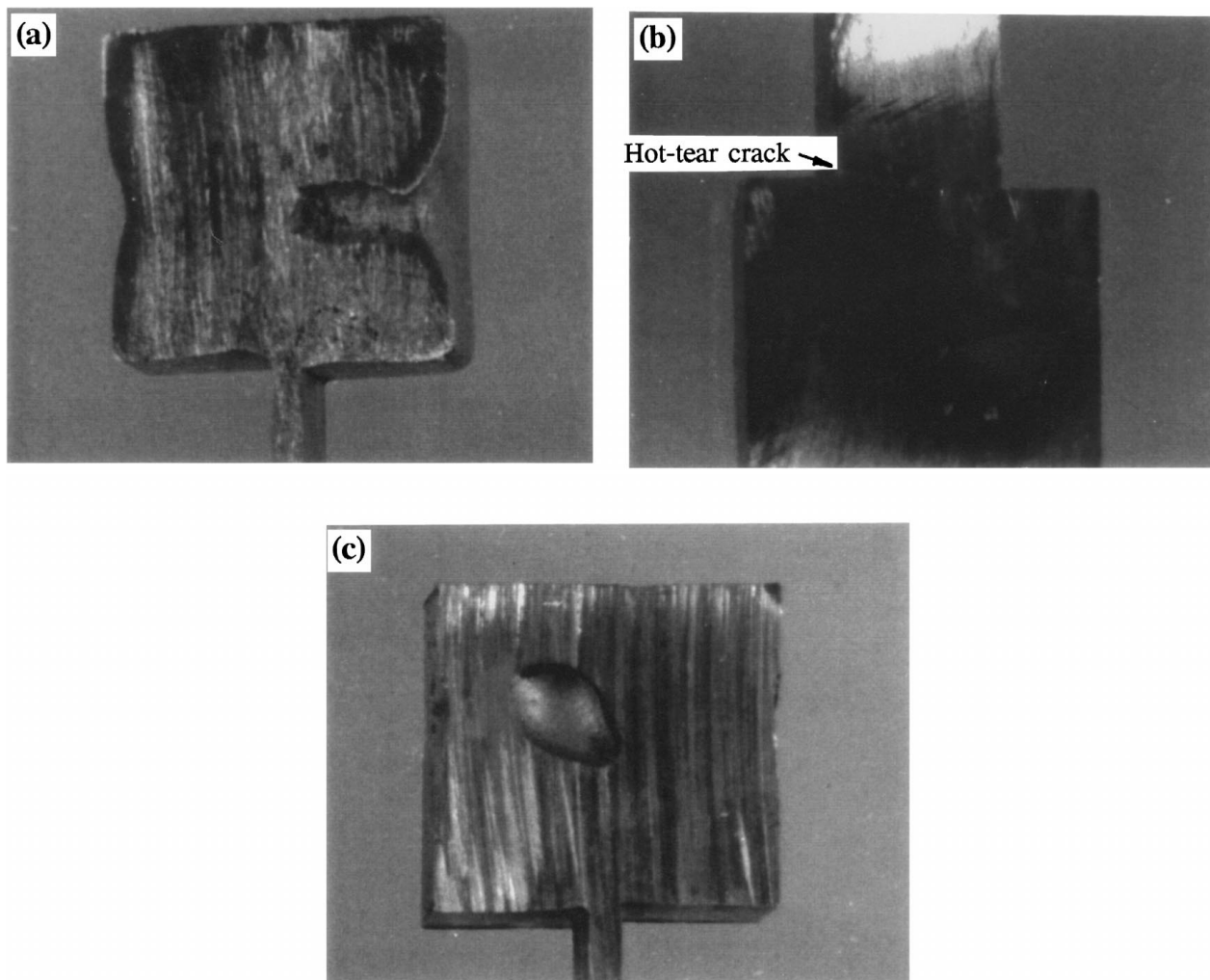


Figure 9 Casting defects; (a) shrinkage porosity in the end section of gravity cast 7050 alloy with a middle section thickness of 2 mm, (b) hot-tear cracks where the middle section joins the base section in gravity cast 7050 alloy with a middle section thickness of 10 mm, and (c) shrinkage porosity in the end section of squeeze cast 7050 alloy with a middle section thickness of 2 mm.

2 mm, see Fig. 9b, and where the base section joins the biscuit section for all middle section thicknesses. With the squeeze cast billets, Fig. 8b, no shrinkage pipe defect or hot-tear cracks were observed, although a shrinkage void ~ 5 mm long was present in the end section of the billet with a middle section thickness of 2 mm, Fig. 9c.

3.3. Microstructure

Fig. 10 shows optical micrographs at the base, middle and end sections for gravity and squeeze cast 7050 alloy billets with a middle section thickness of 20 mm. The cast microstructure of the 7050 alloy consisted of primary Al dendrites and fine intermetallic particles in the eutectic constituent. The squeeze cast billet had a finer microstructure than the gravity cast billet, with a mean Al cell size of $\sim 26.8 \mu\text{m}$ at the middle section of the gravity cast billet, and $\sim 23.9 \mu\text{m}$ at the corresponding middle section of the squeeze cast billet, as shown in Table III. There was also a slight refinement in microstructure from the base section towards the end section of the gravity and squeeze cast billets, see Fig. 10.

Fig. 11 shows corresponding micrographs for gravity and squeeze cast 7050 alloy billets with a middle section

thickness of 2 mm. The microstructure at the middle section of the billets, Figs 11c and d, was finer than for the billets with a middle section thickness of 20 mm, Figs 10c and d. For example, the cell size decreased from ~ 26.8 and $\sim 23.9 \mu\text{m}$ for gravity and squeeze cast billets with a middle section thickness of 20 mm, see Table III, to ~ 16.9 and $\sim 6 \mu\text{m}$ for gravity and squeeze cast billets with a middle section thickness of 2 mm. The middle section had a finer microstructure than the base or end sections for both the gravity and squeeze cast billets.

Fig. 12 shows the primary Al cell size at the middle section as a function of middle section thickness

TABLE III Cell sizes with standard deviations for the middle section of 7050 alloy billets manufactured by gravity casting and indirect squeeze casting

Middle section thickness (mm)	Cell size (μm)	
	Gravity cast	Squeeze cast
20	26.8 (1.7)	23.9 (0.7)
10	23.7 (1.6)	18.7 (0.4)
5	17.5 (1.0)	14.6 (0.1)
2	16.9 (0.5)	6 (0.1)

Gravity Cast

Indirect Squeeze Cast

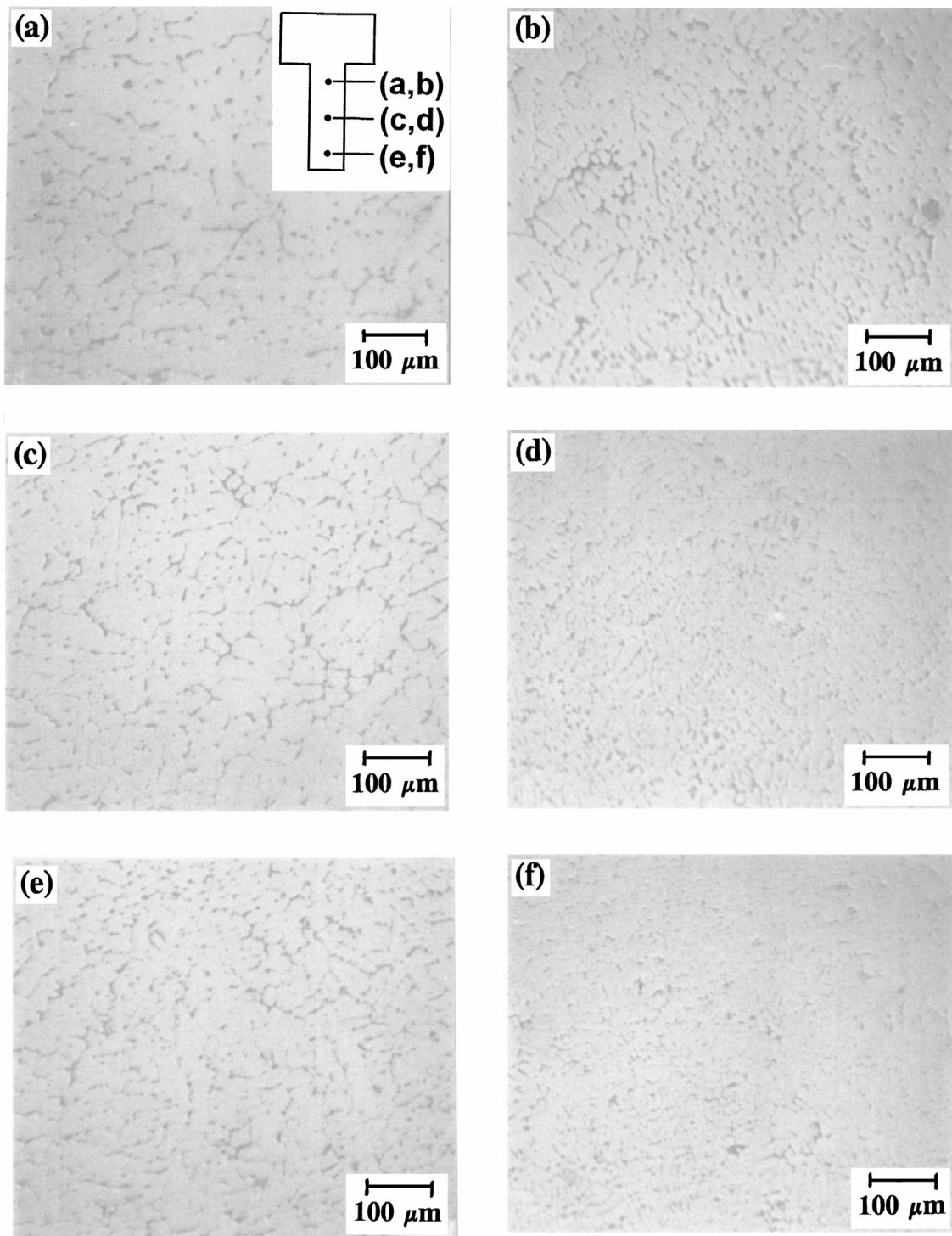


Figure 10 Optical micrographs of 7050 alloy billets with a middle section thickness of 2 mm manufactured by (a, c, e) gravity casting and (b, d, f) indirect squeeze casting, taken from the base section (a, b), middle section (c, d) and end section (e, f).

for gravity and squeeze cast 7050 alloy. The cell size increased with middle section thickness in an approximately parabolic manner, and the cell size was greater for gravity cast material than for squeeze cast material for a given middle section thickness.

Fig. 13 shows optical micrographs from gravity and squeeze cast billets with a middle section thickness of 20 mm, taken from the region where the base section joins the biscuit. In the case of the gravity cast billet, Fig. 13a, a hot-tear formed, running from the surface

towards the centre with a depth of ~ 1 mm. However, no hot-tears formed at the same location in the squeeze cast billet, Fig. 13b. Fig. 14 shows corresponding optical micrographs from the billets with a middle section thickness of 5 mm, taken from the region where the middle section joins the base section. Extensive hot-tear cracks formed in the gravity cast billet, Fig. 13a, running across the entire thickness of the billet, but none formed in the squeeze cast billet, although connected regions of eutectic constituent were present.

Gravity Cast

Indirect Squeeze Cast

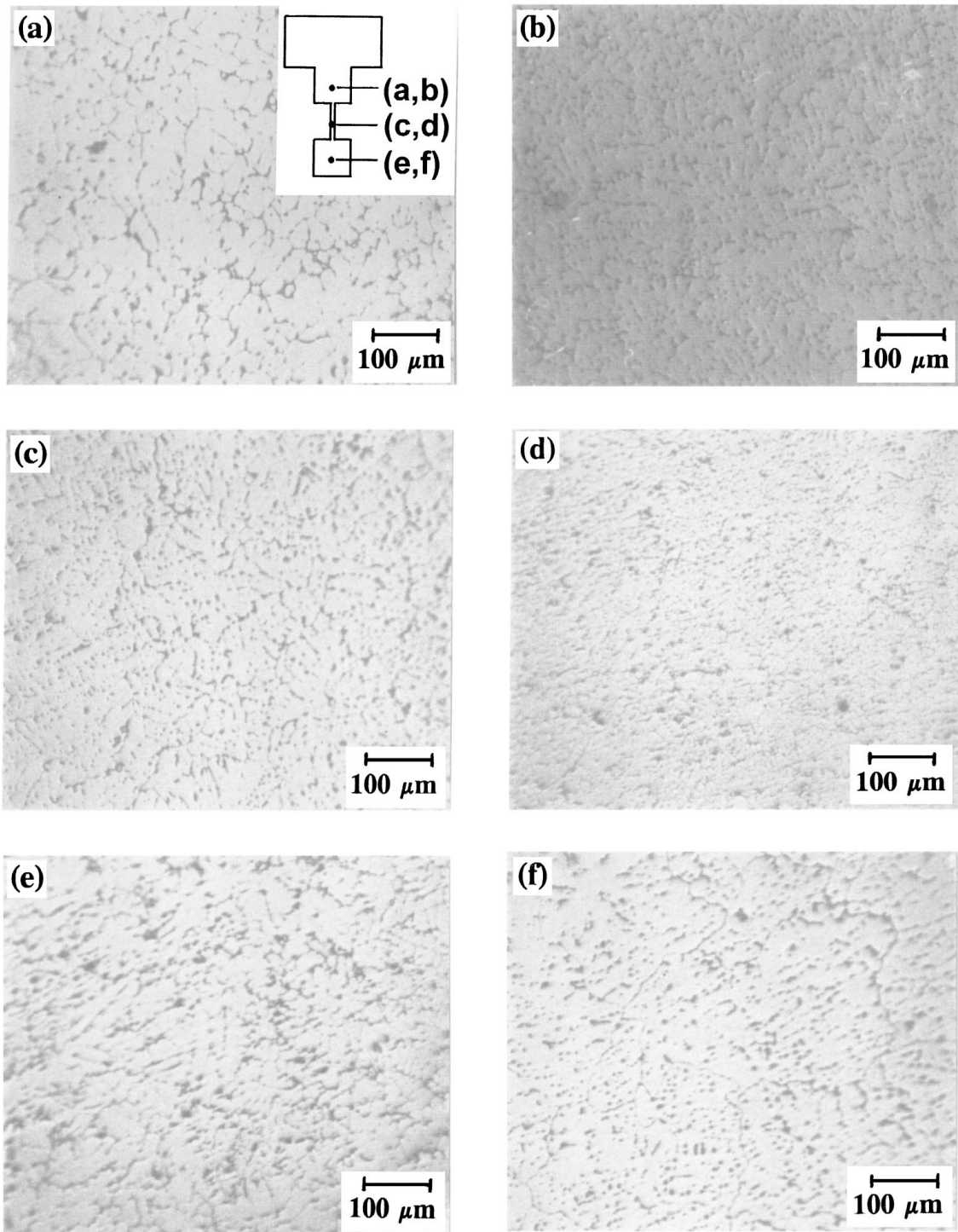


Figure 11 Optical micrographs of 7050 alloy billets with a middle section thickness of 2 mm manufactured by (a, c, e) gravity casting and (b, d, f) indirect squeeze casting, taken from the base section (a, b), middle section (c, d) and end section (e, f).

4. Discussion

4.1. Die replication and macrostructure

Shrinkage contraction, which is $\sim 7\%$ for Al alloys [4], results in poor die replication for gravity cast billets, see Fig. 7, with rounding of the vertices and uneven flat surfaces. However, the application of 50 MPa pressure during squeeze casting results in much better die replication because the pressure forces the melt surface against the die wall throughout solidification.

A number of defects are present in gravity cast billets, see Fig. 9, in particular (1) a shrinkage pipe, (2) shrink-

age voids in the end sections for middle section thicknesses of 5 and 2 mm, and (3) hot-tear cracks where the biscuit joins the base and where the base joins the middle section. The shrinkage pipe is due to the biscuit feeding solidification shrinkage in the remainder of the billet, and the voids in the end section are caused by freezing-off in the relatively thin middle section, which prevents feeding to the end section. For example, for the gravity cast billet with a middle section thickness of 5 mm, the solidification time after the onset of solidification is ~ 18.6 s for the middle section, compared

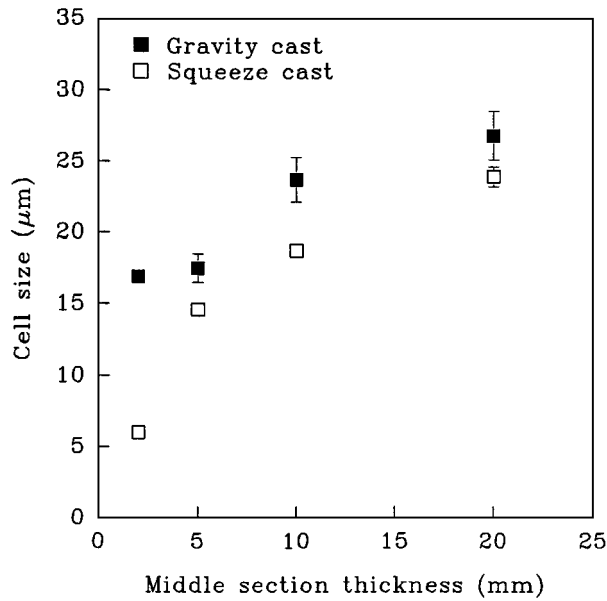


Figure 12 Cell size at the middle section as a function of middle section thickness for gravity and indirect squeeze cast 7050 alloy.

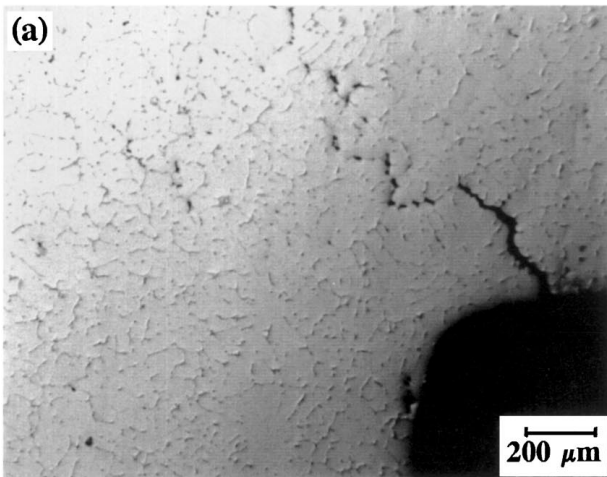


Figure 13 Optical micrographs taken from the region where the base section joins the biscuit section for 7050 alloy billets with a middle section thickness of 20 mm, manufactured by (a) gravity casting and (b) indirect squeeze casting.

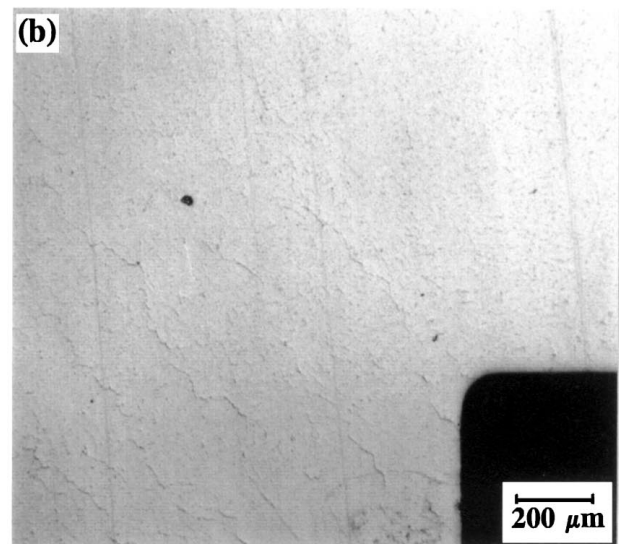
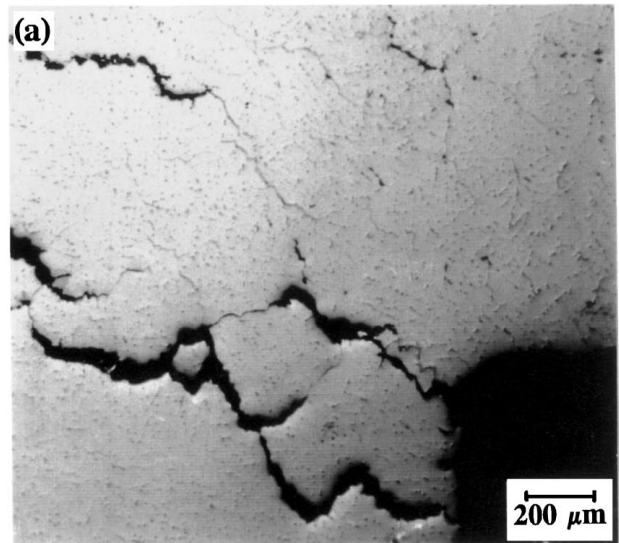


Figure 14 Optical micrographs taken from the region where the middle section joins the base section for 7050 alloy billets with a middle section thickness of 5 mm, manufactured by (a) gravity casting and (b) indirect squeeze casting.

with ~ 23.4 s for the end section, see Table I. The hot-tear cracks are also caused by differences in solidification time between the biscuit, base, middle and end sections of the billet [8]. Considering the hot-tear between the middle and base sections, the middle section solidifies first, such that further shrinkage contraction in the base section results in a stress in the relatively weak semisolid, leading to the formation of a crack. No hot-tear cracks are observed between the end and middle sections, perhaps because the difference in solidification time between the end and middle sections is generally less than for the base and middle sections, see Table II.

Squeeze casting greatly reduces the extent of as-cast defects, see Fig. 7. The shrinkage pipe defect is removed by the action of the ram, which effectively crushes the solidifying shell to give a flat interface between the melt and the end of the ram. Shrinkage voids in the end section are avoided except for the smallest middle section thickness of 2 mm, indicating that with the

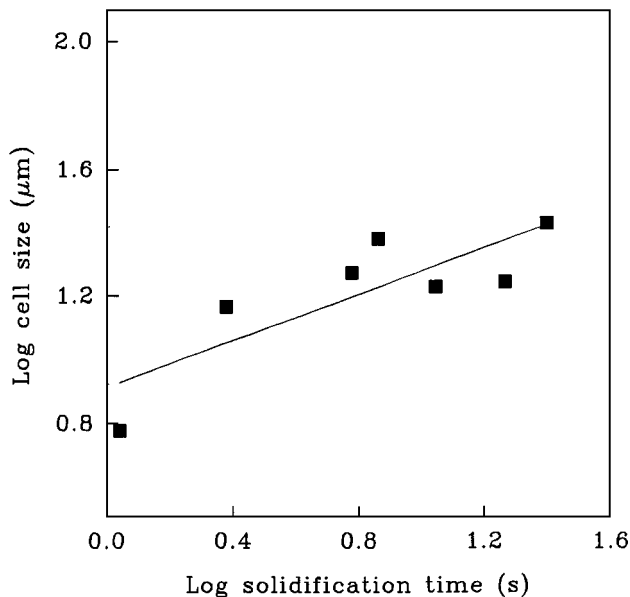


Figure 15 The effect of solidification time after the onset of solidification on the primary Al cell size at the middle section for gravity and indirect squeeze cast 7050 alloy.

larger middle section thicknesses, the pressurised interdendritic fluid can flow through the middle section up to higher solid fractions. Squeeze casting removes the hot-tears observed in the gravity cast billets. This resistance to hot-tearing for squeeze casting is probably due to the high compressive hydrostatic stress component caused by the applied pressure, which suppresses the nucleation of cracks. In addition, the pressurised interdendritic fluid fills any cracks which form, which may explain the connected regions of eutectic observed in the squeeze cast billets, see Fig. 14b.

Squeeze casting results in a refinement of the microstructure when compared with gravity casting, see Figs 10 and 11. For example, the gravity cast billet with a middle section thickness of 10 mm had a primary Al cell size in the middle section of $\sim 23.7 \mu\text{m}$, whereas the corresponding squeeze cast billet had a cell size of $\sim 18.7 \mu\text{m}$, see Table III. This microstructural refinement is due to a decrease in the solidification time [4, 8], which was $\sim 18.6 \text{ s}$ for the gravity cast billet and $\sim 2.4 \text{ s}$ for the squeeze cast billet. The reduction in solidification time is caused by the intimate contact between the melt and die during pressurisation, which leads to a much higher heat transfer coefficient between the melt and die and faster cooling rates [9]. Zhang and Cantor [10] have shown that for an Al-7 wt % Si-0.3 wt % Mg alloy, the melt/die heat transfer coefficient increases from $\sim 2000 \text{ W m}^{-2} \text{ K}^{-1}$ for gravity casting to $\sim 7000 \text{ W m}^{-2} \text{ K}^{-1}$ for squeeze casting at 50 MPa. In addition to the effect of pressure, a decrease in section thickness also leads to a refinement of the microstructure as a result of a reduced solidification time, see Fig. 12.

Fig. 15 shows the effect of solidification time after the onset of solidification on the primary Al cell size at the middle section for gravity and indirect squeeze cast 7050 alloy billets. Relationships between the cell size d and solidification time t for Al alloys have the

form [4, 8]:

$$d = at_f^n$$

where a and n are alloy specific constants. The data from the current work are consistent with this relationship, see Fig. 15, and give an exponent n of approximately 0.4, which is in reasonable agreement with published data for other Al alloy systems where n is usually in the range of 0.33 to 0.5 [4]. However, this value for n has been determined over only a relatively small range of solidification times.

5. Conclusions

1. 7050 Al alloy can be cast to near-net shape with excellent die replication using Indirect squeeze casting. Defects which occur with gravity casting such as a shrinkage pipe, macro-porosity and hot-tearing, are largely removed by squeeze casting, although macro-porosity can re-appear when thick sections are fed through much thinner sections.

2. Squeeze casting results in considerable refinement of the microstructure due to a marked decrease in the solidification time. The decrease in solidification time is caused by intimate contact between the pressurised melt and the die, which leads to an increase in the melt/die heat transfer coefficient. Decreasing the section thickness also results in a refinement of the microstructure due to a reduction in solidification time.

Acknowledgements

The authors would like to acknowledge the RASOM Centre at Chungnam University, Taejon, Korea for funding, and Dr P Evans from Alcan International for supplying the material. We would also like to thank Mr. P. Simmons for assistance with the experimental work and Dr. M. Gallerneault for assistance with the die design.

References

1. G. A. CHADWICK and T. M. YUE, *Met. Mater.* **5** (1989) 6.
2. "Product Design and Specifications for Squeeze Casting" (ELM International Inc., East Lansing, Michigan, USA, 1994).
3. M. GALLERNEAULT, G. DURRANT and B. CANTOR, *Met. Trans. A* **27A** (1996) 4121.
4. J. CAMPBELL, "Castings" (Butterworth-Heinemann Ltd., Oxford, UK, 1991).
5. D. L. ZHANG, C. BRINDLEY and B. CANTOR, *J. Mater. Sci.* **28** (1993) 2267.
6. H. G. KANG, H. I. LEE, P. R. G. ANDERSON and B. CANTOR, in "Proc. Process and Fabrication of Advanced Materials IV," edited by T. S. Srivatsan and J. J. More (TMS, Warrendale, Pennsylvania, 1996).
7. S-W KIM, G. DURRANT and B. CANTOR, *J. Mats. Synth. and Proc.* **6** (1998) 75.
8. M. F. FLEMMINGS, "Solidification Processing" (McGraw-Hill, London, UK, 1974).
9. J. A. SEKHAR, G. J. ABBASCHIAN and R. MEHRABIAN, *Mater. Sci. Eng.* **40** (1979) 105.
10. D. L. ZHANG and B. CANTOR, *Modelling Simul. Mater. Sci. Eng.* **3** (1995) 121.

Received 6 October 1997

and accepted 11 November 1998